Strain-Dependent Cross-Bridge Cycle for Muscle

D. A. Smith and M. A. Geeves
Max-Planck Institute for Molecular Physiology, 44026 Dortmund, Germany

ABSTRACT The cross-bridge cycle for actin, S1 myosin, and nucleotides in solution is applied to the sliding filament model for fully activated striated muscle. The cycle has attached and rotated isomers of each actomyosin state. It is assumed that these forms have different zero-strain conformations with respect to the filament and that strain-free rate constants are the nominal solution values. Only one S1 unit of heavy meromyosin is considered. Transition-state theory is used to predict the strain dependences of S1 binding to actin, the force-generating transition to rotated states, and the release/binding of nucleotide and phosphate. We propose that ADP release and ATP binding are blocked by positive strain and phosphate release by negative strain. At large strains, rapid dissociation of S1 nucleotide from actin is expected when the compliant element of the cross-bridge is strained in either direction beyond its elastic limits. The dynamical behavior of this model of muscle contraction is discussed in general terms. Its computed steady-state properties are presented in an accompanying paper.

INTRODUCTION

Understanding muscle action from a molecular viewpoint requires the synthesis of biochemical, mechanical, and structural approaches. It is generally agreed that the current experimental knowledge of striated muscles is compatible with the sliding filament model (A. F. Huxley, 1957; H. E. Huxley, 1969), but this model is still not fully integrated with biochemical information from solution kinetics and muscle fiber experiments or with the known structures of actin (Kabsch et al., 1990) and myosin S1 (Rayment et al., 1993a,b). Although Huxley's model established the framework for a theory of muscle contraction, the information available from different disciplines has always seemed insufficient for construction of an integrated theory. The experimental systems (proteins, myofibrils, fibers, intact muscles) differ too widely in their degree of organization, and their behavior varies considerably with muscle type (fast, slow, insect flight, cardiac) and experimental conditions (temperature, and ionic strength, pH, nucleotide, and phosphate levels in the sarcoplasm). This variability arises mainly from the various forms of muscle myosin, which are part of a larger family of myosins. However, comparative studies (e.g., Marston and Taylor, 1980) suggest that, at full activation, the same biochemical cycle operates for all muscle types, including smooth muscles.

Cross-bridge models for striated muscle require reaction rates for the biochemical steps to be dependent on elastic strain. The construction of such models is not new, and previous models are discussed in the last section of this paper. Hill (1974) has shown how to make the strain-dependent cross-bridge cycle compatible with chemical thermodynamics by relating strain-dependent equilibrium constants to the standard Gibbs energies of actomyosin states, including elastic cross-bridge energy. The position with respect to the strain dependence of reaction rates is less satisfactory. It has been recognized by some authors that the transition-state theory can be used to construct the strain dependence of transitions involving bound states, but structural assumptions are also required and the theory has rarely been applied in a systematic way. The usual approach is to choose the strain dependence of transitions to fit some experimental data, while keeping the equilibrium constants compatible with thermodynamics.

We believe that the time is ripe to develop a comprehensive cross-bridge theory compatible with the biochemical information and, in a preliminary way, with structural information also. What is different here is that the starting point is a biochemical ATPase cycle based on a few general principles of protein–protein interactions, coupled to a rigorous application of transition-state theory to strain-dependent transitions for the three types of event in the ATP-ase cycle: cross-bridge attachment, cross-bridge "rotation," and ligand dissociation and binding. The biochemical cycle in solution is that proposed by Geeves et al. (1984), the so-called 3G model. In this paper the corresponding tightly coupled model of the cross-bridge cycle is defined by combining this cycle with appropriate structural assumptions about bound states of myosin S1 and actin. The functional forms of the strain dependence of transitions are then fully determined, within a few disposable parameters, by the structural and biochemical bases of the model, especially the existence of well-defined S1 conformations for each bound state and the implication that the set of states in the 3G model is complete.

In its simplest form the model contains only five adjustable parameters (cross-bridge stiffness, cross-bridge throw distance, number of actin sites available, and energy barriers for the release of ADP and phosphate) in addition to the rate constants. Fine tuning of the strain-free rate constants is permissible within the uncertainties of the solution data. However, the latter are sufficiently well constrained that a comprehensive test of this model against observed behavior

Received for publication 24 October 1994 and in final form 3 May 1995.
Address reprint requests to Dr. David Smith, The Randall Institute, King's College London, 26–29 Drury Lane, London WC2B 5RL, UK. Tel.: 71–836-8851; Fax: 71–497-9086; E-mail: dave@muscle.rai.kcl.ac.uk.

0006-3495/95/08/524/14 $2.00

is still likely to generate qualitative disagreements unless the biochemical/structural foundations of the model reflect the actual mechanism. Such failures are important indicators of what structural changes to the model are required: large changes in the values of the structural parameters listed above are trivial examples but by no means the only ones. Thus the success of this model in describing a wide range of muscle behavior is a global test of this version of the sliding filament model. In the accompanying paper (Smith and Geeves, 1995) this is attempted for basic steady-state properties of fully activated muscle. In subsequent papers the model will be applied to transient responses from length and ramp shortenings, small sinusoidal changes in length or pressure, pressure jumps, and the release of caged nucleotides or phosphate. The emphasis in this presentation is on the assumptions underlying the model and how it functions at the molecular level.

UNDERLYING ASSUMPTIONS OF THE 3G MODEL

This model of the biochemical solution cycle will be used as a basis on which to build a mechanical crossbridge model. It was reviewed by Geeves (1991) in the light of more recent biochemical findings, and little has happened since then to alter the underlying principles. The major question is whether this model is sufficient to explain the dynamic behavior of fully activated muscle or whether additional intermediates (such as collision complexes or actomyosin-products complexes) are required for dealing with specific experimental results. Our approach is to keep to the simplest version of the model, as this allows us to set a simple set of rules governing the strain dependence of any cross-bridge transition. We can then see what features of muscle contraction the model is capable of producing.

The 3G model proposes that there are three states of the interaction between actin and myosin heads (Fig. 1). Detached heads initially attach to actin to form the A states (attached) that occur before the generation of net force and then isomerize to the rotated or rigorlike (R) states. In each of these three states the active site of myosin can be empty or occupied by ADP + Pi, ADP, or ATP. In the attached (A) state, ligands bind to the active site in the same way that they bind to free myosin heads. After transition to the R state, actin is bound more tightly and the ligand more weakly. In the absence of nucleotide or in the presence of ADP the equilibrium constant K_2 for the transition is >1, so the R state is preferred. With ADP and Pi bound to myosin, K_2 is not too different from unity, and both A and R states are occupied. However, with ATP bound, $K_2 << 1$ and the A state is favored. Hence the binding and hydrolysis of ATP give a mechanism for cycling between the A and R states. The equilibrium between detached and A states is simply a matter of protein concentration.

We assume that strain-free reaction rates in muscle fibers are equal to those of the isolated proteins in solution under equivalent conditions.

Table 1 lists all rate and equilibrium constants for the 3G model of Fig. 1, intended as a notional set of values for rabbit psoas (fast-twitch) fibers at 20°C. Most values are well defined by existing experiments. It should be noted that collision complexes are omitted from the model. For each actin binding and ligand binding/dissociation reaction there is good evidence for a collision complex preceding the event shown (Geeves, 1991, and references therein), so each reaction is the product of two steps. In most cases the collision complexes are formed rapidly and occur transiently at low occupancy, and their inclusion would make little difference to the modeling. However, in the case of actin binding to M.ATP and M.ADP.Pi there is little direct evidence to distinguish them from the attached states. At physiological salt concentrations these rates are not well defined, and are they set in Table 1 at 10^8 M^{-1} s^{-1}, the notional limit for a diffusion-controlled reaction. Pseudo-first-order binding rates are a function of the effective concentration of actin sites, which in fibers is not a well-defined quantity but is assumed to be 1 mM. All equilibrium constants in the table satisfy detailed balancing and yield an equilibrium constant of 4×10^5 M for the hydrolysis of free ATP, close to the value measured by Alberty (1968).

In this model there are four types of event, namely, cross-bridge binding to an actin site, cross-bridge isomer-

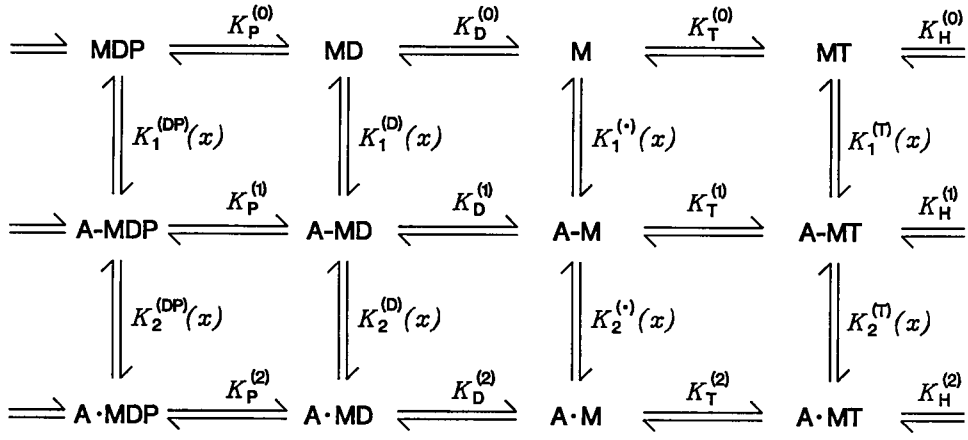

FIGURE 1 States and strain-free transitions of the 3G model; M, S1 myosin; A, actin; T/D, adenosine tri/diphosphate. The three rows give detached, attached and rotated states respectively. Values of all rate and equilibrium constants are given in Table 1.

TABLE 1 Strain-free rate and equilibrium constants, etc. for the 3G model

N	DP	D	—	T
$\tilde{k}_1^{(N)}$ (M^{-1} s^{-1})	2×10^8	4×10^5	4×10^6	1×10^8
$\tilde{K}_1^{(N)}$ (M^{-1})	1×10^4	1×10^4	1×10^5	1×10^4
$k_2^{(N)}$ (s^{-1})	2000	5	500	0.025
$K_2^{(N)}$	1	10	100	5×10^{-6}
i	0 (Detached)	1 (Attached)		2 (Rotated)
$k_P^{(i)}$ (s^{-1})	0.05	0.05		1000
$\tilde{K}_P^{(i)}$ (M)	0.1	0.1		1
$k_D^{(i)}$ (s^{-1})	2.0	2.0		800
$\tilde{K}_D^{(i)}$ (M)	2×10^{-6}	2×10^{-5}		2×10^{-4}
$\tilde{k}_T^{(i)}$ (M^{-1} s^{-1})	1×10^6	1×10^6		1×10^6
$\tilde{K}_T^{(i)}$ (M^{-1})	2×10^{11}	2×10^{10}		1000
$k_H^{(i)}$ (s^{-1})	100	50		50
$K_H^{(i)}$	10	10		2×10^6

In all rates and equation constants the subscript indicates the reaction step (i = 1 for attachment, 2 for rotation, P, D, or T for phosphate or nucleotide release/binding and H for ATP hydrolysis). The superscript specifies a constant condition ($N = DP$, D, null, or T for nucleotide states and i = 0, 1, 2 for the rows of Fig. 2). For computations, $\alpha = kc^2/RT = 4$. $h = c \equiv 5.5$ nm (unit of length), and $\Delta_D = 0.75$ length unit for ADP release and ATP binding. $\Delta_P = 0$ unless declared otherwise. Forced detachment is used with $d_+ = 3.0$, $d_- = -3.5$, and $\beta_1 = \beta_2 = 100$, $k_3 = 5000$ s^{-1} for all attached and rotated states. The same value of k_3 applies for strain-independent detachment from A.MT. Standard concentrations are $[A] = [P] = 1$ mM. $[T] = 5$ mM, $[D] = 30$ μM.

Sources: Geeves (1991) and references therein for the top columns (N = D–T) and D and T ligands of the bottom right column; Trentham et al. (1976) for the bottom–left column. S1 binding for $N = DP$ is assumed similar to $N = T$, and the absence of bound MDP in actin–MDP mixing at low $[A]$ implies that $K_2 \leq 1$. Detailed balance supplies the equilibrium constants for the A-to-R transition with $N = T$, also phosphate release and ATP cleavage on R–states. Ligand rates and equilibria on A–states are assumed similar to those on detached S1. Only k_2 for $N = DP$ and the rate of Pi release from A.MDP are unavailable; they are assigned at 1000 s^{-1} or more for rapid length-step response and high v_0. The rate of hydrolysis from A.MT is presumably slow and therefore noncontributing.

Modifications: S1–actin binding rates for MDP and MT are raised to the limit for a diffusion-controlled reaction. The A → R rate and equilibrium constant with no nucleotide were reduced by factors of 4 and 2, respectively.

ization from the A state to the R state, ligand binding/dissociation events (for ATP, ADP and phosphate), and the bond-breaking ATP cleavage step. The ATP cleavage step on bound states (A or R) is assumed to be strain independent. In the next section we give the structural assumptions of the model and consider how the first three types of events in the biochemical pathway can be affected by strain.

Structural assumptions

The structural assumptions of this model are traditional but should be declared, as they determine the strain dependence of transitions: 1) The A and R states have different zero-strain conformations with respect to the actin filament, which are independent of bound nucleotide or phosphate. 2) A states isomerize to R states by a rotational distortion of the cross-bridge, which produces more tension as the distal part of the cross-bridge is moved along the filament axis by the throw distance $2h$ (nominally 11 nm). 3) Some part of the cross-bridge (S1 or its S2 tail) is elastically compliant in this direction with a finite stiffness k ($4–7 \times 10^{-4}$ N/m), whereas the myosin and actin filaments are treated as rigid structures. 4) Each detached S1 head can explore a small number of binding sites on the actin filament, the precise number being limited by orientational mismatch and the extent of translational fluctuations of S1 in the direction of the filament axis. 5) Adjacent heads do not compete for the same actin binding site. Those on the same thick filament (spaced by 14.3 nm) cannot both address the same actin filament, and those from different thick filaments also have an orientation problem. 6) Finally, to make the theory tractable we assume that, of the two S1 heads of heavy meromyosin bound to the S2 tail, only one is active at any given time, so the presence of a second head is ignored. Experimental support for these statements has been discussed in many places, e.g., Bagshaw (1992). Cooke (1987), and Squire (1994), although direct structural evidence for head rotation and well-oriented attached states in muscle fibers is still lacking.

The next section gives a set of assumptions for translating this kinetic scheme into strain-dependent rate constants for cross-bridges by the transition-state theory.

MINIMAL RULES FOR STRAIN-DEPENDENT CROSS-BRIDGE RATES

What are the simplest reaction pathways that give strain-dependent rate constants? In principle, these paths can be deduced from structural aspects of the model. Then transition-state theory (Glasstone et al., 1941) can be applied straightforwardly, at least on the basis that the rate-limiting step is determined solely by the highest-energy barrier in the pathway as seen from the initial state. This is a simplified version of what is already an approximate theory (Kramers, 1940; Weiss, 1986) but avoids the need to deal with intermediate states, which appear as local energy minima in the optimal path. The transition-state theory is consistent with Gibbs's thermodynamic identity, which relates the strain dependence of any equilibrium constant to the difference in standard Gibbs energies of the initial and final states, including their elastic strain energies (Hill, 1974). Mathematical details of this application are available elsewhere (Wood and Mann, 1981; Smith, 1990a).

Strain-dependent rates are given below for the first three kinds of transition in the 3G model. A fourth subsection considers whether additional detachment pathways are required in the muscle cross-bridge cycle.

Binding to actin

If the most favorable actin site (that with the least mismatch in azimuthal orientation) is displaced by distance x along the filament from the equilibrium position of the detached head, then there is a cost $kx^2/2$ in elastic energy on binding to the

attached state. This energy must be supplied thermally through Brownian fluctuations either in S1 position along the filament axis or in its orientation, depending on whether the elastic element lies in the S2 tail or in the distal neck of each S1. The probability of this fluctuation is proportional to the Boltzmann factor $\exp(-kx^2/2RT)$, where T is absolute temperature and R the Boltzmann constant. In fact there is a preexponential factor dependent on x, and on temperature as in most thermally activated processes. The required probability is of longitudinal S1 fluctuations to all displacements $>x$ (for $x > 0$), assuming that this leads to capture by the actin site at x. In the limit of zero-range forces, the fluctuations preceding capture are force free, and the capture probability is

$$\int_x^\infty \exp(-ky^2/2RT)dy \Big/ \int_0^\infty \exp(-ky^2/2RT)dy$$

$$\approx (2RT/\pi kx^2)^{1/2} \exp(-kx^2/2RT)$$

for $|x| >> (RT/k)^{1/2}$ (both signs of x). Thus the result in Eq. 1 below is correct to logarithmic accuracy within the exponent. Note that x is not, and need not be, distributed. However, if the bound head is orientationally rigid, the only barrier to detachment is the sharp chemical binding well at $\theta = \theta_1$, so the detachment rate would be strain independent. Thus, for orientationally rigid actomyosin, the binding/dissociation rates are given to logarithmic accuracy by

$$k_1(x) = k_1 \exp(-\alpha x^2/2), \quad k_{-1}(x) = k_{-1} \quad (\alpha \equiv k/RT), \quad (1)$$

where k_1 and k_{-1} are the equivalent solution rates. By Gibbs's thermodynamic identity, this Boltzmann factor also appears in the equilibrium constant, so a kinetic interpretation of both rates is unnecessary.

Mechanisms for a strain-dependent detachment rate require structural alterations to the present model, and are considered below and in the concluding discussion.

Attached ⇔ rotated transitions (1 ⇔ 2)

A realistic calculation of the transition state, and hence of the energy barriers separating the A and R states, is beyond the reach of current atomic structure calculations. What is required is the strain dependence of these barriers, which is apparently a yet more difficult problem. However, simple estimates of the strain dependence of the transition state follow naturally from the simple structural postulates of this model, in particular those of orientationally stable A and R states and of the absence of intermediate states (local energy minima) on the A-to-R pathway in solution.

Under isometric conditions the transition must occur at constant x. In this case the reaction coordinate for the path is assumed to be an angle θ describing the orientation of the movable part of acto S1 with respect to the filament axis toward the Z line. Orientationally defined A and R states imply sharp potential wells for these states at $\theta = \theta_1$ and $\theta = \theta_2$, respectively, (90° and 45° in Fig. 2 *A*). If cross-bridges were not tethered, the absence of intermediate states would imply that the Gibbs energy as a function of θ is flat between these wells. The elastic energy of tethered cross-bridges depends on θ and on the strain variable x, giving the reaction energy profiles shown in Fig. 2 *A* for different values of x. There are different forms of angular dependence for the regions $x > 0$ (extension for both states), $-2h < x < 0$ (compression for the A state but extension for the R state) in which there is a zero-strain energy minimum at some intermediate angle of rotation, and $x < -2h$ (both states in compression).

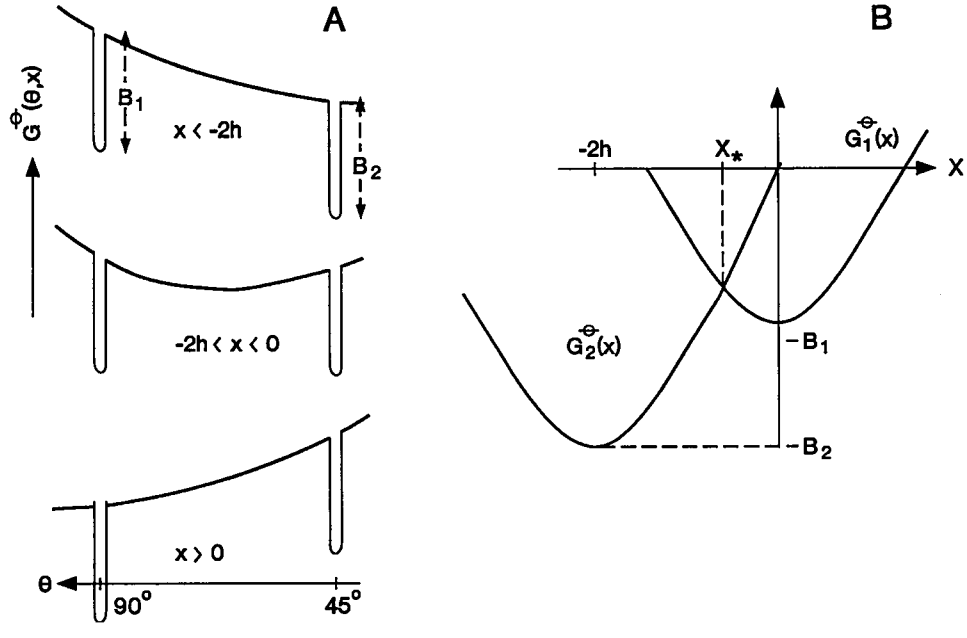

FIGURE 2 (*A*) Gibbs energy $G°(\theta,x)$ of the actomyosin cross-bridge as a function of angle of rotation θ with the filament axis (left-hand diagrams) for various values of actin site displacement x, showing orientationally stable attached and rotated states at 90° and 45°, respectively, with binding energies B_1 and B_2, plus elastic energy $k(x + r\cos\theta)^2/2$, where r is the radius of rotation of the S1–S2 junction. Cross-bridge strain blocks the attached-to-rotated transition when $x, > -h$, where elastic energy is higher in the second state. (*B*) Gibbs energies of the attached and rotated states as functions of x, with zero-strain points at $x = 0$ and $-2h$, respectively. The intersection of the two curves defines the transition point x_*.

Fig. 2 *A* shows that the highest transition state always lies at the top of one potential well. For $x > -h$ the *R* state has higher elastic energy, $k(x + 2h)^2/2$, than the A state, $kx^2/2$, so the transition state is the top of the potential well of the R state and transitions out of the R state are strain independent, whereas transitions in require an additional activation energy, $2kh(x + h)$. For $x < -h$ the A state has more strain energy, so the A-to-R transition is strain independent, whereas the reverse transition requires extra activation energy, $-2kh(x + h)$. Hence

$$k_2(x) = k_2 \exp(-2\alpha h(x + h)), \qquad k_{-2}(x) = k_{-2}, \qquad (x > -h), \tag{2a}$$

$$k_2(x) = k_2, \quad k_{-2}(x) = k_{-2} \exp(2\alpha h(x + h)) \qquad (x < -h), \tag{2b}$$

where k_2 and k_{-2} are the strain-free isomerization rates. The equilibrium constant

$$K_2(x) = k_2(x)/k_{-2}(x) = K_2 \exp(-2\alpha h(x + h)) \tag{3}$$

contains an exponential factor with exponent $2kh(x + h)/RT$ proportional to the difference in elastic energies of states 1 and 2. By Gibbs's identity, this amounts to including elastic energy in the standard Gibbs energy of each state (Hill, 1974).

These statements can be checked against a "cartoon" representation of the strain-dependent A ⇔ R transformation in the top left corner of Fig. 3. This is loosely based on the recent three-dimensional model of the actomyosin complex of Rayment et al. (1993a,b). S1 is shown consisting of three domains, upper jaw (UJ), lower jaw (LJ), and distal (DTL) domains, and a circle denotes one actin site. The geometric arrangement of these domains is subject to thermal fluctuations about the time-averaged structures shown in the left column. Both the A state (top left diagram of Fig. 3) and the R state immediately below are orientationally stable owing to stereospecific binding of domains of S1 to actin (UJ for the A state, LJ also for the R state) and also to binding between the UJ and the DTL, which stabilizes the A state against strain. If these linkages are due to short-range forces, then an A → R transition would break the UJ–DTL link before rotation of the DTL–LJ part and form a LJ–actin link after rotation. Short-range binding forces imply sharp potential wells, of angular width say 1–2° as in Fig. 2 *A*; the curvature of the wells gives the stiffness required for orientationally stable A and R states capable of holding tension against a strained elastic link to the thick filament. The activation energies represented by the depths of these wells are related to the temperature dependence of $k_2 + k_{-2}$. The absence of known intermediates between A and R states implies that, in solution, the reaction energy profile with angle outside the wells has no significant minimum. We assume that the profile is flat on the energy scale $k(2h)^2/2 \approx$ 20 KJ/mol of elastically strained cross-bridges.

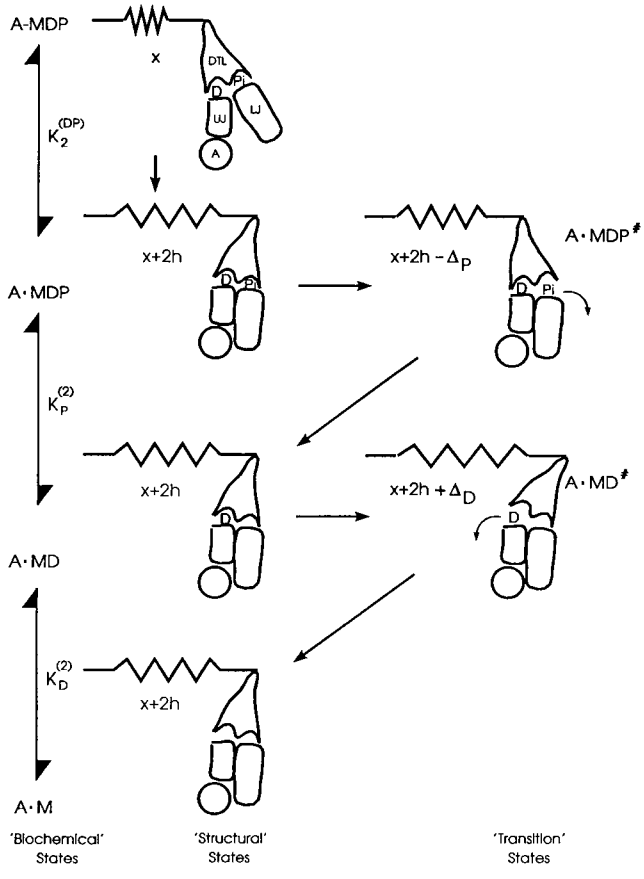

FIGURE 3 Schematic representation of strain-dependent transitions of the bound cross-bridge. The first column shows the main biochemical pathway from the actomyosin A state (A-MDP, with ADP and Pi bound) through isomerization to the R state followed by loss first of Pi and then of ADP. The second column is a representation, based loosely on the model of Rayment et al. (1993a,b), of the types of structural state that could correspond to these biochemical states. The myosin head is shown as consisting of three domains: upper jaw (UJ), lower jaw (LJ) and distal (DTL). Important interactions occur among these three domains, and these interactions are modulated by the nucleotide and Pi binding sites lying between them. *The detached head* (not shown): The ADP and Pi are tightly bound, and interdomain movements are required for release of the the two ligands. These are relatively rare events in the absence of actin. *The A state* is formed by interaction between actin and UJ, and this has little influence on the nucleotide and Pi or on the relationship among the three domains. For simplicity of drawing, the elastic element is shown in the S2 portion of the head but could be within the distal domain or between the domains. The head–S2 junction is displaced by a distance x from its rest position in making the attachment. *The R state:* The transition to the R state involves closing of the jaws and additional interactions between the head and actin. Closing of the jaws produces a displacement of the head–S2 junction by a distance $2h$. Note, however, that the release of ligands is still not possible from this state without further changes in the relationship among the three domains. The remaining states in the second column, are all R states and are structurally identical. *Transition states:* Loss of Pi from A.MDP requires a transient movement of the distal domain away from the lower jaw. Given the geometry of the cross-bridge, this movement is in the direction to reduce cross-bridge strain and so will occur more frequently in positively strained heads. Conversely, after Pi dissociation the loss of ADP requires a transient displacement of the distal domain relative to the upper jaw and will result in additional strain in the cross-bridge. This will therefore occur with lower frequency for cross-bridges already carrying positive strain. As drawn here, the binding of ATP would require a similar distortion of the cross-bridge to allow ATP access to the binding site.

Equations 2a were first used by Huxley and Simmons (1971) to predict fast tension transients from A → R transitions induced by a sudden shortening, which was the first mechanical evidence of these states. More general formulas result if repulsive or "antibinding" barriers between attached and rotated states are included (Smith 1990a); these have the effect of changing the value $x = -h$ that separates the strain-dependent and strain-independent manifolds of each rate function, while maintaining $-h$ as the value of x at which the rates take their strain-free values. In this and the following paper (Smith and Geeves, 1995) there is no need for these modifications.

Strain-controlled ligand dissociation and binding

The extension of the solution rates to muscle fibers requires some form of strain-limited release of products to populate tension-bearing R states. We therefore introduce a "simple" strain dependence of ligand dissociation or binding without requiring any new states or transitions. This can be done by postulating a transition state sensitive to strain. The existence of a transition state for ligand release is not automatic if the initial and final states have the same orientation and hence the same strain energy.

We assume that the transition state for dissociation/binding of the ligand is generated by thermal fluctuations of the protein structure and that the presence of strain in the protein modifies the form of these fluctuations. In the absence of detailed structural information the simplest assumption is that the ligand dissociation pathway is blocked and requires a thermal fluctuation of the structure to allow the ligand to escape. In the absence of strain such fluctuations are frequent and pose no serious impediment to ligand dissociation. Depending on the geometry of the binding site with respect to the direction of strain, strain could either enhance or inhibit the fluctuations that allow the escape of ligand. This is illustrated in its simplest form in Fig. 3.

In the absence of actin, thermal fluctuations allow transient openings of the cleft that allows Pi to dissociate (at a net rate of 0.05 s^{-1}) followed by a similar fluctuation of the cleft that allows ADP release (net rate 2 s^{-1}). The formation of the A state involves stereospecific contact between actin and the UJ but has little influence on the relationship among the three S1 domains and therefore little effect on the rates of Pi and ADP release. Isomerization to the R state, by closing of the "jaws" and formation of additional bonds between actin and the LJ, alters the relationship among the three domains so that the S1–S2 junction is translated by the throw distance $2h$. In the absence of strain this allows both clefts to open more readily and leads to accelerated Pi release followed by accelerated ADP release. The presence of $+ve$ strain on the head inhibits the A-to-R transition, as shown in Fig. 2. In the R state, positive strain in the head will inhibit fluctuations that promote ADP release but should have no effect on the rate of Pi release. Negative strain would have the opposite effect, i.e., inhibition of Pi release only.

Strain-dependent ADP release can now be formulated as follows. Let Δ_D be the displacement of the S1–S2 junction toward the Z line required for ADP release. In the rotated state (A. MD) the initial and final strain energies for this fluctuation are $k(x + 2h)^2/2$ and $k(x + 2h + \Delta_D)^2/2$. Hence the extra energy cost that results from elastic strain is $k\Delta_D(x + 2h + \Delta_D/2)$, which is positive only for large x. The probability of this fluctuation is then reduced by the corresponding Boltzmann factor, but no reduction occurs when this energy difference is negative if the binding well of the initial state is sufficiently narrow. Hence the rate of ADP release from the rotated state (A.MD) is

$$k_D(x) = k_D \exp(-\alpha\Delta_D(x + 2h + \Delta_D/2)) \quad (x > -2h - \Delta_D/2) \quad (4a)$$
$$= k_D \quad (x < -2h - \Delta_D/2).$$

Again note that the strain-free release rate k_D represents the attempt frequency of oscillations in a potential well of the R state (a DTL–LJ link in Fig. 3) multiplied by an Arrhenius escape factor. In this model, escape from the well is a prerequisite for ligand release and for strain control of release when cross-bridge strain raises the energy of the transition state, so large-amplitude orientational fluctuations are required. Only fluctuations that open the cleft lead to ligand release, although fluctuations can occur in both directions. In this model the ADP dissociation constant is strain independent because the initial and final R states have the same elastic energy. Hence the rate $k_{-D}(x)$ of ADP binding to A.M has the same functional dependence on x. For attached states, x should be replaced by $x - 2h$ on the right-hand sides of Eqs. 4a and in the inequalities.

These formulas also apply to ATP binding to the rotated state A.M (and with the same modification to the attached state A-M), probably with the same displacement barrier.

The release of phosphate may also be strain-dependent. Fig. 3 suggests that phosphate release requires the S1–S2 junction to be displaced in the *opposite* sense, by distance Δ_p. Then

$$k_p(x) = k_p \exp(\alpha\Delta_p(x + 2h - \Delta_p/2)) \quad (x < -2h + \Delta_p/2) \quad (4b)$$
$$= k_p, \quad (x > -2h + \Delta_p/2).$$

for release from A.MDP, with the same functional forms for phosphate binding to A.MD and the same modification for release, etc. from the attached state.

In practice, modeling suggests that displacements of 3–4 nm are required for strain-blocked ADP release and ATP binding. Caged ATP-release experiments from strained rigor states (Dantzig et al., 1991) show some evidence of this mechanism. The need for strain blocking of phosphate

release is investigated in the following paper (Smith and Geeves, 1995). The ATP cleavage step on A states of acto-S1 might also be controlled by cross-bridge strain, but simple mechanisms are not obvious, and there is apparently no need.

Additional pathways and the limits of elastic behavior

Suppose that the elastic behavior of the cross-bridge is limited, in extension and compression, to the range $d_- < x < d_+$ of strain values, where $d_- < 0$ and $d_+ > 0$. Without assuming that these limits are necessarily reached in muscle under normal physiological conditions, such limits must exist and are finite. What happens to actin binding and dissociation rates when these limits are reached or (for detached heads) exceeded? If bound heads totally resist attempts to strain them beyond these limits, their elastic energy becomes infinite outside the elastic range. This implies that the binding constant and the rate of binding are both zero, while the dissociation rate is finite, arbitrary (in the sense that it cannot be predicted from the solution rate), but presumably faster than the solution rate. For binding wells of finite angular width the mechanism is the lowering of the energy barrier in the direction of strain (Fig. 2 *A*).

These conclusions apply to attached and rotated states, but note that strain is x for attached and $x + 2h$ for rotated states. At very large x values of either sign, both states will be beyond their elastic limits, forcing detachment from all bound states. However, there is also a region of negative x values in which attached states are forced off but rotated states are not and a similar range of positive values for which the reverse holds. In these regions the rate of isomerization from the stable bound state to the unstable one is obviously zero, whereas the reverse rate is finite, large, and (in the above sense) arbitrary.

Rates for binding/dissociation, A-to-R transitions, and direct dissociation from rotated states are denoted by subscripts ± 1, ± 2, and 3. Beyond elastic limits they become irreversible in the following way:

$$x > d_+, x < d_- - 2h: \quad k_1(x) = 0, \quad k_{-1}(x) = \beta_1 k_{-1}, \quad k_3(x) = k_3, \tag{5a}$$

$$d_- - 2h < x < d_-: \quad k_1(x) = 0, \quad k_{-1}(x) = \beta_1 k_{-1}, \quad k_2(x) = \beta_2 k_2, \quad k_{-2}(x) = 0, \tag{5b}$$

$$d_+ - 2h < x < d_+: \quad k_2(x) = 0, \quad k_{-2}(x) = \beta_2 k_{-2}, \quad k_3(x) = k_3, \tag{5c}$$

where β_1 and β_2 are greater than 1. In Eqs. 5a all states are detached; only attached states are forced off in Eqs. 5b, and rotated states off in Eqs. 5c.

A potential problem with the 3G model is the lifetime of R states at the end of the cycle under rapid shortening. If the detachment pathway is from A.MT to A-MT, then this pathway will be blocked for bridges carried into regions of negative strain (Eqs. 2b), giving a very low unloaded contraction velocity and similar problems with quick-release experiments (Smith 1990b). Hence we have modified the model by allowing strain-independent detachment from the A.MT state at a rate of 5000 s^{-1}. This path would not be evident in solution-kinetic experiments, which cannot distinguish direct dissociation at 5000 s^{-1} from an equally fast indirect process through A-MT. Alternatively, one could make the back rate $k_{-2}(x)$ for the A.MT state strain independent by giving that state a large antibinding barrier. In practice, there would be little difference between these

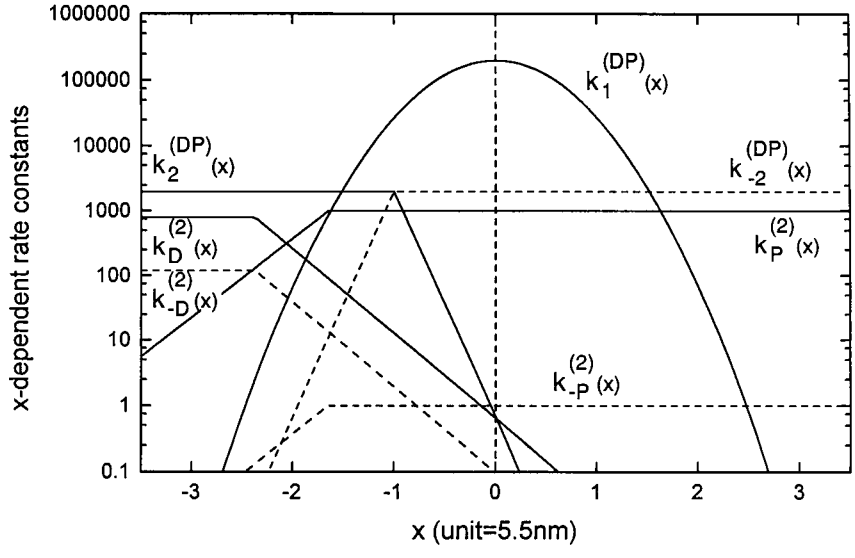

FIGURE 4 Plots of the major strain-dependent rate constants as specified in Table 1 and Eqs. 1–4 against actin site displacement x, using $\alpha = 4$, $h = 1$ unit, and $\Delta_D = 0.75$ unit. Note the logarithmic vertical scale.

alternatives as long as binding of MT to actin remained fast and reversible.

Fig. 4 summarizes strain-dependent reaction rates used in this model for actin binding, isomerization, and ligand binding/release, using a logarithmic vertical scale and the values of Table 1. Mathematical symbols for physicochemical quantities are summarized in Table 2.

OPERATING PRINCIPLES

Molecular motors generate positive isometric tension and directed motion under no load. The direction of motion in muscle fibers and filaments is determined by the polarity of the actin filament (Sellers and Kachar 1990), which dictates the geometry of S1 binding. A key issue is whether tension is generated primarily by one or more power strokes per cycle, by strain-blocked dissociation of positively strained cross-bridges, or both. A discrete power stroke may generate force by rotation of part of the cross-bridge, as suggested by Huxley and Simmons (1971) and Huxley (1974) and identified here with the transition between A and R states observed in solution. Alternatively, net tension in fibers could be generated kinetically by preferential dissociation of negatively strained cross-bridges, without requiring any power-stroke transition in the cross-bridge cycle. Thermal-ratchet models (Vale and Oosawa, 1990; Magnasco, 1994; Astumian and Bier, 1994) are of this kind. To sharpen the distinction, a "pure power-stroke model" is defined as having one or more force-generating transitions but no strain dependence of detachment rates of S1 from actin.

The model presented here is also hybrid but includes pure power-stroke models (by setting $\Delta_P = \Delta_D = \Delta_T = 0$) and pure ratchet models ($h = 0$). How does this model function as a molecular motor? How is this functionality related to the essential features of the model, including the biochemical 3G cycle and the strain dependences implied by orientationally stable A and R states? The main issues are how the hydrolysis of ATP leads to tension in isometric muscle, how tension varies with the velocity of shortening/lengthening, and the efficiency of mechanochemical energy conversion. However, energetics are not considered here. A useful diagnostic available from modeling is how the occupation probabilities of all states vary with strain in all circumstances.

TABLE 2 Mathematical symbols used

α	kc^2/RT = ratio of elastic to thermal energies (Eqs. 1)
b	Half-pitch of actin double-helix
β_1	Large-strain enhancement factor for S1 binding to actin
β_2	Enhancement factor for A–R transitions
c	Actin site spacing
d_1, d_2	Half-widths for binding curves of A and R states versus strain
d_-, d_+	Strain values for onset of forced (large-strain) detachment
($\Delta_d = \Delta_T$), Δ_P	Displacement distortions for opening nucleotide, Pi clefts
$2h$	S1 throw distance in A–R transition
$J(x)$	ATPase flux thru cycle from heads with strain x
k	Stiffness per cross-bridge (bound S1)
$k_X^{(Y)}$, $k_{-X}^{(Y)}$	Forward/backward strain-free rate constants (see Table 1)
$k_X^{(Y)}$, $k_X^{(Y)}(x)$	Strain-free/strain-dependent rate constants
$K_X^{(Y)}$, $K_X^{(Y)}(x)$	Strain-free/strain-dependent equilibrium constants
$p_1(x)$, $p_2(x)$	Binding probabilities of A and R states (1 and 2)
R	Boltzmann's constant (gas constant if per mole)
R	ATPase rate/S1 head
T	Absolute temperature
T	Tension per thin filament
θ_1, θ_2	S1 orientations in A and R states
θ	S1 orientation (general)
v_0	Unloaded contraction velocity per half-sarcomere
x	Actin site displacement = strain in A–state
$x + 2h$	Strain in R state
x_+, x_-	Upper and lower limits to binding curve with respect to x in activated muscle (A and R states, respectively)
x_*	Value of x separating A and R states

Cross-bridges are formed by thermal fluctuations

In striated muscle the vernier effect caused by the different spacings (42.9 and 38.5 nm) of detached S1 heads and actin sites along their filaments creates the longitudinal mismatch x (Fig. 4). In this model, heads bind to an attached state of fixed orientation (notionally 90°; Fig. 2 *A*) of one domain of S1, which costs elastic energy unless $x = 0$. This energy must be supplied by thermal fluctuations and produces attached cross-bridges in a range $|x| \leq d_1$, where $d_1 = \sqrt{2RT \ln K_1/k}$. This follows when the strain-dependent binding constant is set at $K_1(d_1) = 1$, where $K_1(x) = K_1 \exp(-kx^2/2RT)$ and K_1 is the strain-free first-order binding constant (Eqs. 1). With k = 0.54 pN/nm, T = 293 K, and a second-order binding constant of 10^4 M^{-1}, $K_1 = 10$ for an effective actin concentration of one mM, so $d_1 = 5.9$ nm. If only one actin site per half-pitch is available, then ~30% of all heads bind, as their x values are distributed over 38.5 nm. More heads bind if cross-bridge stiffness is lower, the number being proportional to $k^{-1/2}$.

Note that reversible binding to the attached state, with no further reaction steps, produces equal numbers of cross-bridges of positive and negative tension, because the equilibrium binding probability is strain dependent by means of elastic potential energy only. This is true regardless of the strain dependence of the binding rate or of whether the elastic element obeys Hooke's law. Hence no isometric tension, and no directed motility, would be produced if subsequent steps in the cycle were blocked. This is confirmed experimentally in relaxed fibers at low ionic strength where the regulated thin filament blocks the A-to-R transition but not S1 binding to the A state (Chalovich and Eisenberg, 1982; McKillop and Geeves, 1992). The viscoelastic behavior of relaxed fibers under these conditions (Brenner et al., 1982) estimates S1 binding rates $\approx 10^4$ s^{-1}, comparable with those for the isolated proteins.

In active muscle the cross-bridge cycle is far from equilibrium

That the cross-bridge cycle is far from equilibrium in active muscle can be demonstrated by comparing active muscle with rigor. In the absence of all nucleotides and phosphate, muscle enters the rigor condition, for which the available S1 states are just M. A-M, and A.M in this model. There is no continued expenditure of chemical energy, so the distributions of these states should eventually approach thermal equilibrium. The equilibrium bound-state distributions are

$$p_1(x) = \frac{K_1 \exp(-kx^2/2RT)}{1 + K_1 \exp(-kx^2/2RT) + K_1K_2 \exp(-k(x+2h)^2/2RT)}, \quad (6a)$$

$$p_2(x) = \frac{K_1K_2 \exp(-k(x+2h)^2/2RT)}{1 + K_1 \exp(-kx^2/2RT) + K_1K_2 \exp(-k(x+2h)^2/2RT)}, \quad (6b)$$

with subscripts 1 and 2 for A and R states, respectively. The net tension

$$T = \frac{1}{b}\int_{-b/2}^{b/2} \{kxp_1(x) + k(x+2h)p_2(x)\}dx \quad (7)$$

is identically zero, as expected for a state of thermodynamic equilibrium. The fact that, in fibers, S1 heads are tethered to the thin filament may appear to violate ergodic conditions (i.e., conditions of access) for thermodynamic equilibrium. However, the vernier effect achieves the same effect by introducing a static disorder in the position of actin sites.

Fig. 5 shows the occupation probabilities of the A and R states versus strain, using the actin site spacing $c = 5.5$ nm as a unit of length. If these distributions did not overlap, they would be symmetric about their respective points of zero strain $x = 0$ and $-2h$, with half-widths d_1 and d_2. Binding considerations give the estimate $d_2 = \sqrt{2RT \ln (K_1K_2)/k}$, which is larger than d_1 when $K_2 > 1$. With $K_2 = 100$ (Table 1), $d_2 = 1.86$ units of length (10.4 nm). However, the distributions of A and R states overlap when $d_1 + d_2 > 2h$, which is true here and expected in general. For given x the dominant state depends on whether the strain-dependent isomerization constant (Eq. 3) is above or below unity, so the division occurs at $x = x_*$, where $K_2(x_*) = 1$. This marks the strain at which the Gibbs energies of the A and R states are equal (Fig. 2 *B*).

In fact, equilibrium is an extreme form or rigor that is never reached in practice. Where the transitions can be followed, solution-kinetic experiments indicate that rotated states never form directly but only through the attached intermediate. This is immaterial to the form of the equilibrium distributions in Eqs. 6, but it does control the time of approach to equilibrium (Fig. 5) through $k_1(x)$, which is a Gaussian function of x (Eqs. 1). Even with the maximum unstrained binding rate of 10^5 s^{-1}, the time of formation of negatively strained R states soon becomes prohibitively large as x falls below -2 units. Thus rigor states formed after depletion of ATP in the presence of Ca^{2+} should be time-dependent nonequilibrium states whose tension decreases as more negatively strained heads bind into the R state.

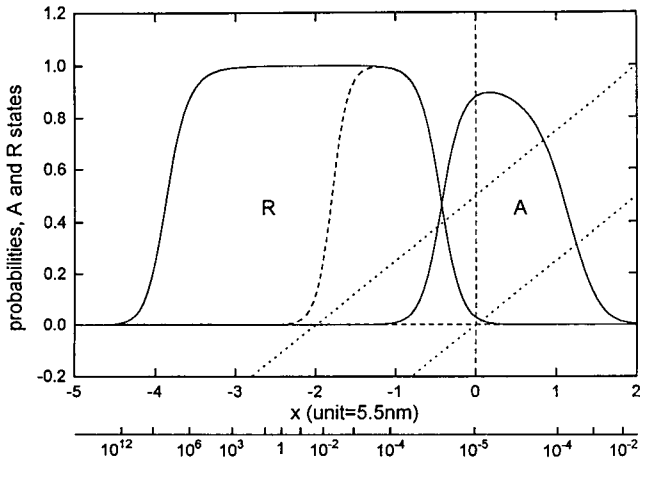

FIGURE 5 Probabilities of (A) attached and (R) rotated states of actomyosin in thermodynamic equilibrium at various strains, and the time scale required for equilibrium to be established. Qualitatively, the effect of adding ATP is to remove R states with strains less than $x_- \approx -2$ units (-11 nm). The dotted lines are tensions (not to scale) for the A and R states.

ATP acts as a chemical ratchet to make tension

When millimolar ATP is added to a fast muscle in rigor, tension rises and after 30–100 ms reaches an active steady state that hydrolyzes ATP at a rate of several s^{-1} per head (e.g., see Goldman et al., 1982). ATP binds rapidly to rigor heads and dissociates them from actin. This process would deplete almost all rotated states unless some mechanism existed to block the ATP-induced dissociation of R states with positive tension ($x > -2h$) while maintaining it to remove negatively strained states. The mechanism that we have proposed (strain blocking of ADP release and ATP binding) does this by truncating the left-hand edge of the distribution of rigor states at $x = x_-$ ($x_- \geq -2$; Fig. 5). Under isometric conditions the depleted states come from detached heads that first bind to A states at large negative strains. Thus they are generated by thermal fluctuations and removed biochemically (at $\sim$5000 s^{-1}). Removal by ATP is irreversible because the unstrained Gibbs energy of A.M + T is higher than that of A + MT by 11.5RT (the overall dissociation constant is 10^5 under physiological conditions.) Thus ATP acts in conjunction with strain-dependent S1

binding to actin as a thermochemical ratchet (see also Vale and Oosawa, 1990).

Note that nearly all this irreversibility is in the head-rotation step, as $K_2 \approx 10^{-5}$ in the presence of ATP and $K_2 \approx 100$ for rigor heads. Hence the ratchet-releasing action of ATP requires both attached and rotated states. This huge reduction in K_2 for the ATP-bearing state of acto S1 is associated with a very large affinity of free myosin S1 for ATP (Table 1), for which there is a loss of negative charge (Bartels et al., 1993).

Inasmuch as ATP-induced detachment is irreversible, tension-generating states must be maintained. This occurs mainly by the hydrolysis of the terminal phosphate group from ATP bound to detached heads, but there is also a return path by binding of M.T into an attached state before hydrolysis. At physiological levels of nucleotide and phosphate the major tension-generating state turns out to be A.MD. The left-hand edge of the strain distribution of A.MD is estimated by setting the escape rate (through ADP release and ATP binding) equal to the rate of regeneration through ATP hydrolysis and binding of A.MDP to actin, assuming that the subsequent steps are fast. Thus

$$\frac{1}{k_D(x)} + \left(1 + \frac{1}{K_D}\right)\frac{1}{k_T(x)} = \frac{1}{k_H} + \left(1 + \frac{1}{K_H}\right)\frac{1}{k_1(x)} \quad (8)$$

determines x_-. In isometric muscle, the dominant reaction cycle in Fig. 1 is MT ⇔ MDP ⇔ A-MDP ⇔ A.MDP ⇔ A.MD ⇔ A.M ⇔ A.MT ⇔ MT, as envisaged by Hibberd and Trentham (1986).

In isometric muscle, not all bound heads hydrolyze ATP

The strain-blocking mechanism for ADP release means that the distribution of A states is little affected by ATP. If x_+ and x_* mark the right- and left-hand edges of the distribution of the A-MDP state, both are well estimated by equilibrium considerations. Thus $K_1^{(DP)}(x_+) = 1, K_2^{(DP)}(x_*)(1 + K_p^{(2)}(x_*)) = 1$, giving

$$x_+ = \sqrt{2 \ln K_1^{(DP)}/\alpha}, \quad (9a,b)$$

$$x_* = -h + \frac{1}{2\alpha h} \ln(K_2^{(DP)}(1 + K_p^{(2)}))$$

(all rate constants are first order). For Table 1, $x_+ = 1.07$ and $x_* = -0.14$ in units of 5.5 nm. Note that the rotated state includes A.MD and A.MDP and that $K_p^{(2)}$ is inversely proportional to phosphate concentration.

Although actin is an effector of the hydrolysis of ATP on myosin, the average ATPase rate/head in fibres, as measured by rates of product release, is much smaller than for S1 and F-actin in solution at saturating concentrations of actin, even although the equivalent actin concentration in fibers is very high. This is attributable to cross-bridge strain, which prevents attached heads in the range $x > x_*$ from rotating to the R state. Thus ATPase in fibers arises only from the rotated heads ($x_- < x < x_*$). In this region the steady-state ATPase flux $J(x)$ is given by

$$\frac{1}{J(x)} \approx \frac{1}{k_H} + \left(1 + \frac{1}{K_H}\right)\frac{1}{k_1(x)} + \frac{1}{k_D(x)} + \left(1 + \frac{1}{K_D}\right)\frac{1}{k_T(x)}, \quad (10)$$

neglecting attached states. Thus the rate-limiting step is strain-blocked ADP release near the right-hand end of this range, but at the left-hand end ATP cleavage from MT or even the binding of the product state to actin is slower. The net rate/head is the average of $J(x)$ over x in $(-b/2, b/2)$, where $b \equiv 38.5$ nm is the actin site periodicity.

Thus all bound heads contribute (nearly all of them positively) to the net tension, but only rotated heads contribute to ATPase, so the isometric "tension cost" (net ATPase rate/tension) is low. The average ATPase rate for *cycling* heads is larger than the rate averaged over all heads in the sarcomere, usually by a factor of 10. However, there are ATP cleavage pathways from detached and attached states of MT (Webb et al., 1986). ATP cleavage in the rotated state can safely be neglected because the A.MT state is populated only at negative strains where ligand release and ATP binding are fast compared with the putative rate of cleavage.

Strain-blocked ADP release controls the behavior of rapidly shortening muscle

The unloaded contraction velocity v_0 of a fully activated muscle is determined by a balance of positive and negative tension contributions from heads of various strains, as confirmed recently by Seo et al. (1994). Under shortening, the isometric distributions in Fig. 5 are distorted and dragged to the left by a distance ≈(shortening velocity) × lifetime. Hence tension-bearing states are forced into negative tension at small x, while the right-hand edge of the distribution is less affected (Huxley 1957). If such states are short lived, then a bigger speed of shortening is required for sufficient negative tension for net cancellation, giving a larger unloaded shortening velocity. In the present model, attached states are not affected by motion if their rate of dissociation and rebinding is sufficiently rapid, above 10^4 s^{-1}. Under these conditions, v_0 is controlled primarily by the rate of escape from the (rotated) A.MD state, which is limited by the rate of ADP release, as proposed by Siemankowski et al. (1985). In this way observed values of v_0 can be reproduced if ADP release at negative strains ($x < -2h$) is not strain blocked, which is achieved for moderate values of Δ_D.

The unblocking of ADP release and ATP binding at negative strains causes the net ATPase rate to rise with shortening velocity v (the Fenn effect). At velocities above $0.5v_0$ the ATP turnover rate starts to level off and may reach

a shallow maximum at velocities below v_0 (Kushmerick and Davies, 1969; Barclay, et al., 1993). Mechanisms for ATPase inhibition in rapidly shortening muscle are still controversial, but the most obvious rate-limiting process is ATP hydrolysis from M.T, which in shortening muscle must take place before the head in question has moved on to the next set of actin sites on the thin filament. Strain-blocked phosphate release at negative strains as proposed here is another possibility, and so is the forced detachment of A.MD heads at large negative strains.

Models without forced detachment are said to be tightly coupled if all cycling heads (here those in the range $x_- < x < x_+$) hydrolyze one molecule of ATP per cycle of binding to and dissociation from actin. This feature is maintained in the 3G model in spite of the presence of extra detachment pathways from the A.MD and A.M states: the rate of back isomerization to A-MD is very slow, and the back rate to A-M is much slower than the rate of ATP binding to A.M at millimolar levels of ATP.

Forced detachments occur in rapidly extending muscle

Under steady-state conditions tension rises rapidly with extension speed and then saturates or falls slightly (Lombardi and Piazessi, 1990; Harry et al., 1990). Conventional cross-bridge theories do not predict the second observation, because the ADP-release/ATP-binding/detachment pathway for rotated states is not available at positive strains. Backrotation to an attached state is not strain blocked at positive strains (in fact, for $x > -h$ in the formulation of the last section), but for A.MD this process is limited by the rate of phosphate binding, which in the present model is very slow at $[P] = 1$ mM. Taking all factors into account, it appears that conventional tightly coupled models cannot avoid generating a huge rise in tension with increasing extension velocity, at least at low concentrations of phosphate. Thus heads must be forced to detach at large positive strains. A mechanism for doing this was suggested in the previous section.

This process generates an accumulation of M.D heads at large positive values of x. Because x is periodic modulo h, the same is true at large negative values, as the extending filaments soon move them onto the next set of actin sites where they bind into the attached A-MD state. Kinetic data of the 3G model (Table 1) show that there is insufficient time for them to rotate before they traverse the binding range, so that the model predicts that tension in rapidly extending muscle is carried by this *attached* state.

CONTEXT

The utility of this model may be clarified by a brief discussion of its relation to other models of the cross-bridge cycle. Models can be classified according to their mechanisms for isometric tension (power stroke or thermal ratchet), by the presence of A and R states (here taken as synonymous with low- and high-force states or weak- and strong-binding states), by the extent to which they can be mapped to some form of the biochemical cross-bridge cycle, and by the level of integration of the strain dependence of transitions with mechanical/structural aspects of the model. Curiously, nearly all pre-1990 models are hybrids or can be interpreted as such. The cycle in Huxley's sliding filament model (Huxley A. F., 1957) contains only one bound state, but the strain dependence of its attachment rate allows only positively strained heads to bind, giving positive net isometric tension. The bound state can be interpreted as an equilibrium mixture of A and R states, which leads naturally to three-state models (e.g., see Julian et al., 1974; Nishiyama et al., 1977) with one A state, one R state, and an explicit power stroke. Huxley's model also contains a ratchetlike action of ATP in the sense that dissociation is more rapid at negative strains, although the x dependence is not continuous ($g_2 > g_1$).

Integration with the actomyosin ATPase cycle started by including the ATP cleavage step on detached heads (Eisenberg et al., 1980). This model also had one A state and one R state. Since then, models evolved by introducing R states with different nucleotides (Wood and Mann, 1981; Smith, 1990b). Models with rotated A.MDP, A.MD, and A.M states have been used by Pate and Cooke (1989) to explore the nucleotide and phosphate dependence of steady-state properties. The attached A-MDP state is on the main pathway, and the fraction of bound states in the A form under various conditions has been subjected to experimental tests under conditions of zero-load (Brenner and Eisenberg, 1986) and low ionic strength (Brenner et al., 1982). Modeling can play an important role by predicting behavior produced by this A state, particularly as it has not been detected by direct probes. The other A states have not been included in these models, but all will be required. The attached A-MT state defines a recognized second pathway for ATP cleavage (Webb et al., 1986; Stein et al., 1979). Very low levels of ATP generate quasi-rigor states in which A.M carries tension and the backrotation path to A-M seen in solution studies may be faster than ATP binding. The attached A-MD state is expected to carry tension whenever heads are forcibly detached by strain, which is suggested as a method of achieving loose coupling (Higuchi and Goldman, 1991; Lombardi et al., 1992; Podolsky and Nolan, 1972; Yanagida, 1990). A comprehensive three-line model was suggested by Eisenberg and Hill (1985) and computationally tested in some areas by Propp (1986); this model did not include strain control of ligand release. A model with strain-controlled ADP release, phosphate release before head rotation, and no explicit A.MD state was used by Smith (1990b), in which the testing of pre-1990 models is summarized. The standard model proposed by Hibberd and Trentham (1986) should be adequate at full activation whenever tight coupling is appropriate.

Strain dependences chosen for the A-to-R transition in most models usually follow Huxley and Simmons (1971),

which correspond to a generalized form of Eqs. 2 with a large antibinding barrier on the R state to keep $k_{-2}(x)$ flat. The treatment of strain-dependent S1 binding and ligand release often uses ad hoc forms that may not be related to any particular mechanism. An exponential dependence of release rate on x was first used by Nishiyama et al. (1977) without justification. The challenge is therefore to find more ways of testing the strain dependences proposed here that represent specified mechanisms.

It is particularly important to test the strain-blocked ADP release mechanism of this paper against models with a piecewise-constant rate of escape. A model of this kind was recently used by Cooke et al. (1994) in conjunction with a cycle including two A.MD states. A second A.MD state has been proposed by Sleep and Hutton (1980) and by Taylor (1991), but there is no consensus on whether this state exists or is on the main pathway in muscle fibers. At 10°C the proposed isomerization rate (60 s^{-1}) is rate limiting for detachment and slow enough to mimic a slow muscle unless some method exists for faster detachment at the negative strains generated by more rapid shortening. At 20°C, Ma and Taylor (1994) give a much higher value (400 s^{-1}), which approaches values reported for the ADP release step by Siemankowski et al. (1985). Thus a loose-coupling model, in which such heads are forcibly detached, was explored by Cooke et al. (1994) as a method of raising the unloaded shortening velocity to values found in fast muscles (2.5–4 (μm/s)/half-sarcomere) and simultaneously inhibiting ATP turnover. This test of the present model, in its tight-coupling form and without a second column of A.MD states, is made in the companion paper (Smith and Geeves, 1995). Transient properties such as length steps and sinusoidal muscle stiffness as a function of frequency also provide searching tests, to be explored in later papers.

Until recently, existing models have not been able to establish whether the release of inorganic phosphate occurs before or after the A-to-R transition. The rate of Pi release from the attached A-MDP state has not been measured but should be slow, as ligand reaction rates on attached states are expected to be close to those on detached heads. Thus the force-generating event should precede phosphate release, although the very high binding constant (~1 M) for Pi prevents the kinetics from being explored in solution. The caged-Pi release experiments of Dantzig et al. (1992) lead to this conclusion, which we confirm in the companion paper by calculating the phosphate dependence of isometric tension. The form of the 3G model is computationally convenient for exploring multiple pathways, e.g., for Pi release and binding.

Alternative cross-bridge cycles that still fit the general framework of the sliding filament model may be generated by changing the structural assumptions, the number of distinct states in the cycle, or the allowed transitions between them. For example, probes using fluorescent labels (Yanagida, 1984) and spin labels (Cooke et al., 1984; Fajer et al., 1990; Thomas, 1994) on S1 suggest that the A states of actomyosin are not orientationally well defined. The experiments are not conclusive, as these probes do not have lifetimes long enough to average over fluctuations on time scales above 10 μs, and they may not be located on the S1 domain stereospecifically bound to actin in the A state. Electron cryomicroscopy (Walker et al., 1994) and x-ray studies (Martin-Fernandez et al., 1994) also suggest a wide range of S1 orientations in active muscle within the resolution of the data. Thus models with variable-angle attachment of S1 to actin may be required, as suggested by Huxley and Kress (1985) and Squire (1994). However, the A-to-R transition would then be energetically less favorable, as the total change $k(x + 2h)^2/2$ in strain energy is always positive. Model calculations of the phosphate dependence of isometric tension should also discriminate between these two kinds of A state.

The 12 states of the 3G cycle are the minimum number required to give attached and rotated states for each bound nucleotide/phosphate combination. The existence of collision complexes for ligand binding to S1 and for S1 ligand binding to actin has already been mentioned. Their presence may affect the dependence of the overall binding rate on nucleotide/phosphate concentration, although the overall equilibrium constant is unchanged. For example, an S1 actin collision complex preceding the A state could permit very rapid initial binding with a slower second step, which could be important in raising the speed of unloaded shortening. This collision state might form over a range of angles with the filament axis. Collision complexes would need to be included explicitly in a generalized 3G model if they open up new pathways or are populated under conditions not found in solution.

The location of the elastic element of the cross-bridge cycle is still uncertain. The present model permits elastic compliance in S2, in the distal part of S1, or both, but also uses dynamic short-range links between the different domains of S1 and between S1 and actin. Orientationally well-defined conformations of some S1 domains is guaranteed in proportion to the stiffness of these links, which is assumed to be much higher than that of the "elastic element." The possibility of models with more compliant links to actin or within S1 was first raised by Eisenberg et al. (1980), although tension production would be more difficult. One effect of increasing the angular width of the S1-actin potential wells would be to raise the detachment rate in proportion to absolute strain $|x|$, because the top of the well would be reduced on one side. The drop in energy barrier can be estimated at $k|x|r\theta_o$, where θ_o is the half-width of the well and r the radius of head rotation, raising the detachment rate by a factor $\exp(k|x|r\theta_o/RT)$. With the values of Table 1 and x = 10 nm, the enhancement factor is $\exp(21\theta_o) = 6$ for $\theta_o = 5°$. Thus large strains can increase the detachment rate of S1 from actin, and the rate of back rotation from the R state, by no more than a factor of 10 with this mechanism. This is not enough to depopulate the A.MD state at large strain, as the strain-free backrotation rate is below 1 s^{-1} (Table 1). Thus a

sudden stiffening of the elastic element seems to be the only way of detaching A.MD heads before ADP release at large strains.

In the same vein, mechanical experiments should be reinterpreted to allow for the compliance of the actin filament, now estimated at 40% of the total sarcomeric compliance (Goldman and Huxley, 1994, and references therein). The stiffness controlling angular fluctuations of the nucleotide or phosphate clefts may not be identical to that controlling the A-to-R transition, as we assumed in deriving Eqs. 4, but changes here could be absorbed in the displacements Δ_D, etc. Finally, the cross-bridge cycle should be enlarged to take into account the two heads of HMM.

In papers to follow, the present model will be tested by its quantitative predictions for many specific phenomena. The formulation and testing of models with different structural assumptions is beyond the scope of this study, although structurally different models generated by changing the five basic non-kinetic parameters are still open.

Note added in proof—After the Biophysical Society discussion meeting in October 1994 [*Biophys. J.* 68 (Suppl.)], the relationship between the domains of myosin and the force generation mechanism may be clearer and consistent with the outline we propose in Fig 3. Yount et al. (44S–49S) suggest that Pi could leave myosin from the opposite side of the myosin head from where ATP enters, i.e., myosin is a "back-door enzyme." Fisher et al. (19S–28S) present additional structural data and propose that the formation of the strong binding state (R-state) of actomyosin would involve a translation and rotation of the lower domain (LJ) of the 50-K segment relative to the upper domain (UJ), closing the cleft between them. These authors believe that the question of which "jaw" binds first to actin to form the A-state is still open, whereas Holmes (2S–7S) suggests that the lower domain binds first. For the general model presented here, these details are not critical but they do suggest that Fig. 3 is consistent with the structural data.

REFERENCES

Alberty, R. A. 1968. Effect of pH and metal ion concentration on the equilibrium hydrolysis of adenosine triphosphate to adenosine diphosphate. *J. Biol. Chem.* 143:1337–1343.

Astumian, R. D., and M. Bier. 1994. Fluctuation driven ratchets: molecular motors, *Phys. Rev. Lett.* 72:1766–1769.

Bagshaw, C. R. 1994. Muscle Contraction, 2nd ed. Chapman & Hall, London.

Barclay, C. J., J. K. Constable, C. J. Gibbs. 1993. Energetics of fast- and slow-twitch muscles of the mouse. *J. Physiol. (London).* 472:61–80.

Bartels, E. M., P. H. Cooke, G. F. Elliott, and R. A. Hughes. 1993. The myosin molecule—charge response to nucleotide binding, Biochimica et Biophysica Acta 1157:63–73.

Brenner, B., and E. Eisenberg. 1986. Rate of force generation in muscle: correlation with actomyosin ATP-ase activity in solution. *Proc. Natl. Acad. Sci. USA.* 83:3542–3546.

Brenner, B., M. Schoenberg, J. M. Chalovich, L. E. Greene, and E. Eisenberg. 1982. Evidence for cross-bridge attachment in relaxed muscle at low ionic strength. *Proc. Natl. Acad. Sci. USA* 79:7288–7291.

Chalovich, J. M., and E. Eisenberg. 1982. Inhibition of actomyosin ATPase activity by troponin-tropomyosin without blocking the binding of myosin to actin. *J. Biol. Chem.* 256:575–578.

Cooke, R. 1987. The mechanism of muscle contraction. *Crit. Rev. Biochem.* 21:53–118.

Cooke, R., M. S. Crowder, C. H. Wendt, V. A. Barnett and D. D. Thomas. 1984. Muscle cross-bridges: do they rotate? *In* Contractile Mechanisms in Muscle, G. Pollack and H. Sugi, editors. Plenum Publishing Corp., New York.

Cooke, R., H. White, and E. Pate. 1994. A model of the release of myosin heads from actin in rapidly contracting muscle fibers. *Biophys. J.* 66: 778–788.

Dantzig, J. A., Y. E. Goldman, N. C. Millar, J. Lacktis, and E. Homsher. 1992. Reversal of the cross-bridge force-generating transition by photogeneration of phosphate in rabbit psoas muscle fibres. *J. Physiol. (London).* 451:247–278.

Dantzig, J. A., M. G. Hibberd, D. R. Trentham, and Y. E. Goldman. 1991. Cross-bridge kinetics in the presence of MgADP investigated by photolysis of caged ATP in rabbit psoas muscle fibres. *J. Physiol. (London).* 432:639–680.

Eisenberg, E., and T. L. Hill. 1985. Muscle contraction and free energy transduction in biological systems. *Science.* 227:999–1006.

Eisenberg, E., T. L. Hill, and Y. D. Chen. 1980. Cross-bridge model of muscle contraction. *Biophys. J.* 29:195–227.

Fajer, P. G., E. A. Fajer, and D. D. Thomas. 1990. Mosin heads have a broad orientational distribution during isometric muscle contraction: time-resolved EPR studies using caged ATP. *Proc. Natl. Acad. Sci. USA.* 87:5538–5542.

Geeves, M. A. 1991. The dynamics of actin and myosin association and the cross-bridge model of muscle contraction. *Biochem. J.* 274:1–14.

Geeves, M. A., R. S. Goody, and H. Gutfreund. 1984. Kinetics of acto-S1 interaction as a guide to a model for the crossbridge cycle. *J. Muscle Res. Cell Motil.* 5:351–361.

Glasstone, S., K. J. Laidler, and H. Eyring. 1941. The Theory of Rate Processes. McGraw Hill, New York.

Goldman, Y. E., M. G. Hibberd, J. A. McCray, and D. R. Trentham. (1982). Relaxation of muscle fibres by photolysis of caged ATP. *Nature (London).* 300:701–705.

Goldman, Y. E., and A. F. Huxley. 1994. Actin compliance: are you pulling my chain? *Biophys. J.* 67:2131–2136.

Harry, J. D., A. W. Ward, N. C. Heglund, D. L. Morgan, and T. A. McMahon. 1990. Crossbridge cycling theories cannot explain high-speed lengthening behavior in frog muscle. *Biophys. J.* 57:201–208.

Hibberd, M. G., and D. R. Trentham. 1986. Relationships between chemical and mechanical events during muscle contraction. *Ann. Rev. Biophys. Biophys. Chem.* 15:119–161.

Higuchi, H. and Y. E. Goldman. 1991. Sliding distance between actin and myosin filaments per ATP molecule hydrolysed in skinned muscle fibres. *Nature (London).* 352:252–254.

Hill, T. L. 1974. Theoretical formalism for the sliding filament model of contraction of striated muscle, part I. *Prog. Biophys. Molec. Biol.* 28: 267–340.

Huxley, A. F. 1957. Muscle structure and theories of contraction. *Prog. Biophys. Biophys. Chem.* 7:255–318.

Huxley, A. F. 1974. Muscular contraction. *J. Physiol. (London).* 243:1–43.

Huxley, A. F., and R. M. Simmons. 1971. Proposed mechanism of force generation in striated muscle. *Nature (London).* 233:533–538.

Huxley, H. E. 1969. The mechanism of muscular contraction. *Science.* 164:1356–1366.

Huxley, H. E., and M. Kress. 1985. Crossbridge behaviour during muscle contraction. *J. Muscle Res. Cell Motil.* 6:153–161.

Julian, F. J., K. R. Sollins, and M. R. Sollins. 1974. A model for muscle contraction in which cross-bridge detachment and force generation are distinct. *Proc. Cold Spring Harbor Sympos. Quant. Biol.* 37:685–688.

Kabsch, W., H. G. Mannherz, D. Suck, E. F. Pai, and K. C. Holmes. 1990. Atomic structure of the actin: DNase I complex. *Nature (London).* 347:37–44.

Kramers, H. A. 1940. Brownian motion in a field of force and the diffusion model of chemical reactions. *Physica.* 7:284–304.

Kushmerick, M. J., and R. E. Davies. 1969. The chemical energy of muscle contraction II. The chemistry, efficiency and power of maximally working sartorius muscles. *Proc. R. Soc. London Ser. B.* 174:315–353.

Lombardi, V., and G. Piazessi. 1990. The contractile response during steady lengthening of stimulated frog muscle fibres. *J. Physiol. (London).* 443:141–171.

Lombardi, V., G. Piazessi, and M. Linari. 1992. Rapid regeneration of the actin-myosin power stroke in contracting muscle. *Nature (London).* 355:638–641.

Ma, Y-Z, and E. W. Taylor. 1994. Kinetic mechanism of myofibril ATPase. *Biophys. J.* 66:1542–1553.

Magnasco, M. O. 1994. Forced thermal ratchets. *Phys. Rev. Lett.* 71: 1477–1481.

Marston, S., and E. W. Taylor. 1980. Comparison of the myosin and actomyosin ATPase mechanisms of the four types of vertebrate muscle. *J. Mol. Biol.* 139:573–600.

Martin-Fernandez, M. L., J. Bordas, G. Diakun, J. Harries, J. Lowy, G. R. Mant, A. Svenson, and E. Towns-Andrews. 1994. Time-resolved X-ray diffraction studies of myosin head movements in live frog sartorius muscle during isometric and isotonic contractions. *J. Muscle Res. Cell Motil.* 15:319–348.

McKillop, D., and M. A. Geeves. 1992. Regulation of the acto-myosin subfragment I interaction by troponin/tropomyosin. *Biochem. J.* 279: 711–718.

Nishiyama, K., H. Shimizu, K. Kometani, and C. Shigeru. 1977. The three-state model for the elementary process of energy conversion in muscle. *Biochim. Biophys. Acta.* 460:523–536.

Pate, E., and R. Cooke. 1989. A model of cross-bridge action: the effects of ATP, ADP and Pi. *J. Muscle Res. Cell Motil.* 10:181–196.

Podolsky, R. J., and A. C. Nolan. 1972. Muscle contraction transients, cross-bridge kinetics and the Fenn effect. *Proc. Cold Spring Harbor Symp. Quant. Biol.* 37:661–668.

Propp, M. B. 1986. A model of muscle contraction based upon component studies. *In* Lectures on Mathematics in the Life Sciences. Vol. 16. American Mathematic Society Providence, 61–119.

Rayment, I., H. M. Holden, M. Whittaker, C. B. Yohn, M. Lorenz, K. C. Holmes, and R. A. Milligan. 1993a. Structure of the actin-myosin complex and its implications for muscle contraction. *Science.* 261: 58–65.

Rayment, I., W. R. Rypniewski, K. Schmidt-Bäse, R. Smith, D. T. R. Tomchick, M. M. Benning, D. A. Winkelmann, G. Wesenberg, and H. M. Holden. 1993b. Three-dimensional structure of myosin subfragment-1: a molecular motor. *Science.* 261:50–58.

Sellers, J. R., and B. Kachar. 1990. Polarity and velocity of sliding filaments: control of direction by actin and of speed by myosin. *Science.* 249:406–408.

Seo, J. S., P. C. Krause, and T. A. McMahon. 1994. Negative developed tension in rapidly shortening whole frog muscles. *J. Muscle Res. Cell Motil.* 15:59–68.

Siemankowski, R. F., M. O. Wiseman, and H. White. 1985. ADP dissociation from actomyosin subfragment 1 is sufficiently slow to limit the unloaded shortening velocity in vertebrate muscle. *Proc. Natl. Acad. Sci. USA.* 82:658–662.

Sleep, J. A., and R. L. Hutton. 1980. Exchange between inorganic phosphates and adenosine 5′-triphosphate in the medium by actomyosin subfragment I. *Biochemistry* 19:1276–1281.

Smith, D. A. 1990a. The theory of sliding filament models for muscle contraction II. Biochemically-based models of the contraction cycle. *J. Theor. Biol.* 146:157–175.

Smith, D. A. 1990b. The theory of sliding filament models for muscle contraction III. Dynamics of the five-state model. *J. Theor. Biol.* 146: 433–466.

Smith, D. A., and M. A. Geeves. 1995. Strain-dependent cross-bridge cycle for muscle. II. Steady-state behavior. *Biophys. J.* 69. In press.

Stein, L. A., R. P. Schwarz, P. B. Chock, and E. Eisenberg. 1979. Mechanism of actomyosin triphosphatase. Evidence that adenosine 5′-triphosphatase hydrolysis can occur without dissociation of the actomyosin complex. *Biochemistry.* 18:3895–3909.

Squire, J. 1994. The actomyosin interaction—shedding light on structural events: "Plus ca change, plus c'est la meme chose," *J. Muscle Res. Cell Motil.* 15:227–231.

Taylor, E. W. 1991. Kinetic studies on the association and dissociation of myosin subfragment 1 and actin. *J. Biol. Chem.* 266:294–302.

Thomas, D. D. 1993. Blitz and blizzard: crossbridges and chaos. *Biophys. J.* 65:21–22.

Trentham, D. R., J. F. Eccleston, and C. R. Bagshaw, 1976. Kinetic analysis of ATP-ase mechanisms. *Q. Rev. Biophys.* 9:217–281.

Vale, R. D., and F. Oosawa. 1990. Protein motors and Maxwell's demons: does mechanochemical energy transduction involve a thermal ratchet? *Adv. Biophys.* 26:97–134.

Walker, M., H. White, B. Belknap, and J. Trinick. 1994. Electron cryomicroscopy of acto-myosin-S1 during steady-state ATP hydrolysis. *Biophys. J.* 66:1563–1572.

Webb, M. R., M. G. Hibberd, Y. E. Goldman, and D. R. Trentham. 1986. Oxygen exchange between Pi in the medium and water during ATP hydrolysis mediated by skinned fibres from rabbit skeletal muscle. *J. Biol. Chem.* 261:15557–15564.

Weiss, G. H. 1986. Overview of theoretical models for reaction rates. *J. Stat. Phys.* 42:3–36.

Wood, J. E., and R. W. Mann. 1981. A sliding-filament cross-bridge ensemble model of muscle contraction for mechanical transients. *Math. Biosci.* 57:211–263.

Yanagida, T. 1984. Angles of fluorescently labeled myosin heads and actin monomers in contracting and rigor stained muscle fibers. *In* Contractile Mechanisms in Muscle, G. Pollack and H. Sugi, editors. Plenum, New York.

Yanagida, T. 1990. Loose coupling between chemical and mechanical reactions in actomyosin energy transductions. *Adv. Biophys.* 26:75–95.